OCEAN COMMUNITY CONFERENCE '98

Celebrating 1998 International Year of the Ocean

THE MARINE TECHNOLOGY SOCIETY

Annual Conference

Baltimore Convention Center
November 16 – 19, 1998

Conference Proceedings

REPORT DOCUMENTATION PAGE

Form Approved
OBM No. 0704-0188

1. AGENCY USE ONLY *(Leave blank)*	2. REPORT DATE	3. REPORT TYPE AND DATES COVERED
	November 1998	Proceedings

4. TITLE AND SUBTITLE

Time-Frequency Analysis of Acoustic Imagery for Bottom Mapping

5. FUNDING NUMBERS

Job Order No. 745703A8

Program Element No.

Project No.

Task No.

Accession No.

6. AUTHOR(S)

Maria T. Kalcic, *Andrew B. Martinez, and Douglas N. Lambert

7. PERFORMING ORGANIZATION NAME(S) AND ADDRESS(ES)

Naval Research Laboratory
Marine Geosciences Division
Stennis Space Center, MS 39529-5004

8. PERFORMING ORGANIZATION REPORT NUMBER

NRL/PP/7441--98-0009

9. SPONSORING/MONITORING AGENCY NAME(S) AND ADDRESS(ES)

Office of Naval Research
Washington, DC 20375-5320

10. SPONSORING/MONITORING AGENCY REPORT NUMBER

11. SUPPLEMENTARY NOTES

Proceedings of the Marine Technology Society Annual Conference, 16-19 November 1998, Baltimore, MD
*Tulane University, EECS Department, New Orleans, LA 70118

12a. DISTRIBUTION/AVAILABILITY STATEMENT

Approved for public release; distribution is unlimited.

12b. DISTRIBUTION CODE

13. ABSTRACT *(Maximum 200 words)*

Acoustic imagery generated by the Naval Research Laboratory's ASCS (Acoustic Sediment Classification System) is analyzed using time-frequency methods. The ASCS Imagery is generated using normal-incidence acoustic data. Nonlinearities in the propagating medium produce multiple harmonics in the return. Different components of the bottom and sub-bottom produce different spectral signatures, based on the harmonics that can be used to classify the bottom. Although the exact acoustic properties of the media may not be known, it is possible to segment the spectrally different components. This paper presents an efficient method for performing the time-frequency analysis. The tradeoffs between time and frequency resolution are examined and exploited to produce the best overall resolution. Examples using the ASCS data demonstrate its use for classification of acoustic imagery. Buried pipes, methane gas deposits, and other features can be differentiated using this method.

14. SUBJECT TERMS	15. NUMBER OF PAGES
acoustic imagery, ASCS (Acoustic Sediment Classification System), and ELAC LSE-179	6
	16. PRICE CODE

17. SECURITY CLASSIFICATION OF REPORT	18. SECURITY CLASSIFICATION OF THIS PAGE	19. SECURITY CLASSIFICATION OF ABSTRACT	20. LIMITATION OF ABSTRACT
Unclassified	Unclassified	Unclassified	SAR

TIME-FREQUENCY ANALYSIS OF ACOUSTIC IMAGERY FOR BOTTOM MAPPING

Maria T. Kalcic[1] and Andrew B. Martinez[2] and Douglas N. Lambert[3]

Abstract— **Acoustic imagery generated by the Naval Research Laboratory's ASCS (Acoustic Sediment Classification System) is analyzed using time-frequency methods. The ASCS imagery is generated using normal-incidence acoustic data. Nonlinearities in the propagating medium produce multiple harmonics in the return. Different components of the bottom and sub-bottom produce different spectral signatures, based on the harmonics that can be used to classify the bottom. Although the exact acoustic properties of the media may not be known, it is possible to segment the spectrally different components. This paper presents an efficient method for performing the time-frequency analysis. The tradeoffs between time and frequency resolution are examined and exploited to produce the best overall resolution. Examples using the ASCS data demonstrate its use for classification of acoustic imagery. Buried pipes, methane gas deposits, and other features can be differentiated using this method.**

I. Introduction

A need exists for detailed mapping of the seafloor prior to dredging operations and the laying of pipelines and cables. In addition, there is a need to be able to precisely locate existing buried pipeline and cable assets in the area so that they are not damaged during the new operations. The location and positive identification of these man-made buried objects can often be difficult because they can be masked in the subbottom imagery by natural sediment structures, methane gas pockets, and man-made discarded trash. However, we have found that the use of a high frequency, short pulse and nonlinearities in the transmitting medium produce a broadband signal that can be exploited to better distinguish between these objects. This paper describes how these properties can be enhanced using time-frequency approaches.

[1]Naval Research Laboratory, Code 7441, Stennis Space Center, MS 39529

[2]Tulane University, EECS Department, New Orleans, LA 70118

[3]Naval Research Laboratory, Code 7431, Stennis Space Center, MS 39529

II. Background

The narrow beam, short pulse and wide bandwidth of the ASCS have shown excellent results in the determination of detailed subbottom structure and prediction of geoacoustic properties [1-3] as well as the detection of buried objects such as pipelines in the upper few meters of the seafloor. Fig. 1 shows an oil pipeline, 0.51 m in diameter, buried in one meter of sand, detected with the ASCS. The pipeline has an extended reverberation tail due to ringing inside the pipe. Also visible in the image are sediment disturbances due to trenching, seen directly above the pipeline in Fig. 1 as sort of 'V' shaped dark area. Remnants of the trenching berms are evident above and to either side of the trench. Many of the returns from muddy sediments, however, are embedded with methane gas bubbles that display a strong acoustic impedance similar to those of the buried objects causing false alarms if the system were used for buried object detection. It is necessary to develop techniques that can distinguish hard reflectors, such as gas pockets, from pipelines and cables, in order to automate the process of object location.

III. Broadband ASCS Acoustic Imagery

Acoustic imagery of a sediment cross-section is produced with a single, normal incident, narrow beam (12 degrees) pinging along a fixed line. The ASCS transducer used in this study, an ELAC LSE-179, produces a

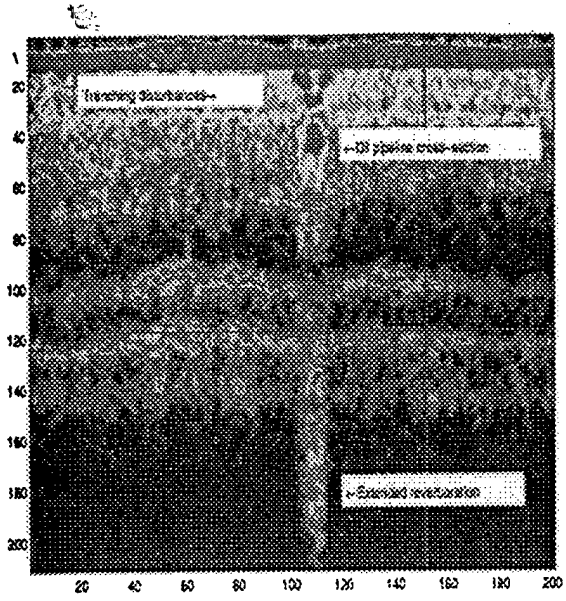

Fig. 1. Oil pipeline detected by ASCS at 15kHz showing extended reverberation tail, and sediments disturbed by trenching operations.

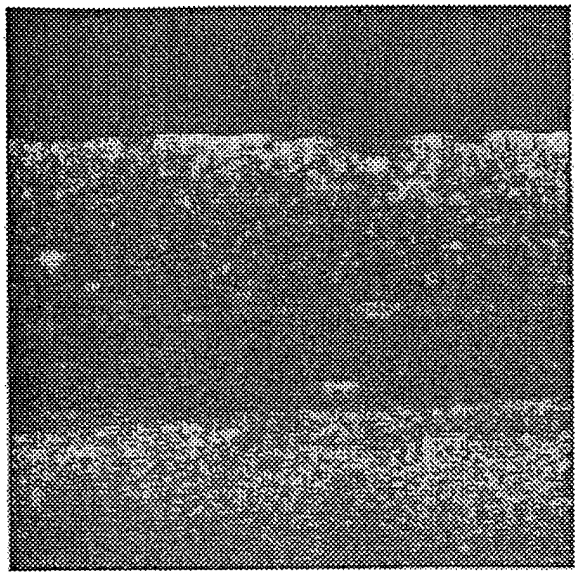

Fig. 2. Several hundred pings from the ASCS with intensity in dB

short 15 kHz pulse that results in a broadband signal, with high time resolution. Sixteen bit data provide approximately 90 dB of dynamic range.

The acoustic imagery generated by the ASCS contains reflections from many objects with the same amplitude making them indistinguishable. Often the problem of distinguishing methane gas deposits from oil pipelines or other objects is very difficult to the trained viewer, and much more so to an automated detection system. Fig. 2 shows a log-intensity image of several hundred pings stacked as columns to produce a single image with depth increasing from top to bottom. Methane gas pockets, surface debris and a buried cable are visible in the image. The log-intensity is used so that some of the less reflective materials are more visible. The bright object in the middle left of the image is a buried cable. As one can see, other objects in the image appear very similar and it is difficult to differentiate the cable from the methane at the bottom of the image or seashell debris at the surface.

The shortcoming of this approach is evident by looking at one column (ping) from Fig. 2. Figure 3 shows the broadband instantaneous intensity of the time sequence of one ping. The largest peak corresponds to the buried cable. The initial large peak represents seashell clutter at the surface and the peaks near the bottom (around samples 550-600) represent methane gas pockets. Since this shows the time varying intensity for all frequencies, differentiation of objects based on different frequency characteristics is not possible, and all processing must be purely spatial.

IV. Narrow-band Processing

The transmission of a 31.25 kHz signal with a 15-kHz piezometer transducer produces harmonics in the received signal due to nonlinearities in the transmission medium. This, combined with the use of a short pulse (0.13 ms), results in a broadband spectrum with strong peaks at several frequencies. It turns out that different materials respond quite differently to the transmitted signal, suggesting an investigation into the spectral character of the returns.

Fig. 4 shows the spectrum of one ping

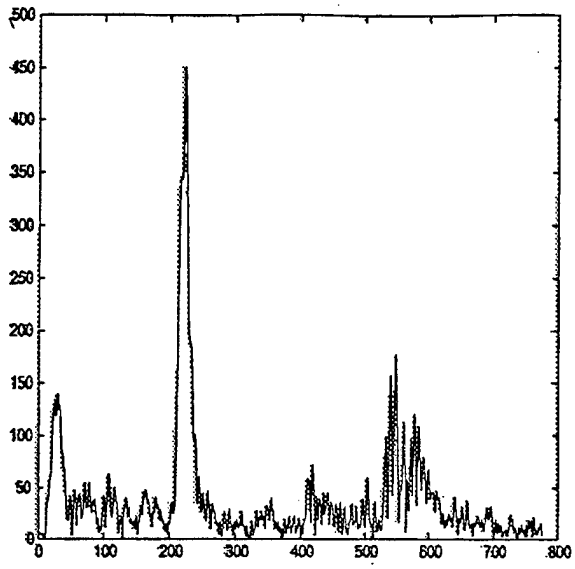

Fig. 3. Instantaneous broadband intensity of a single ping through area of interest.

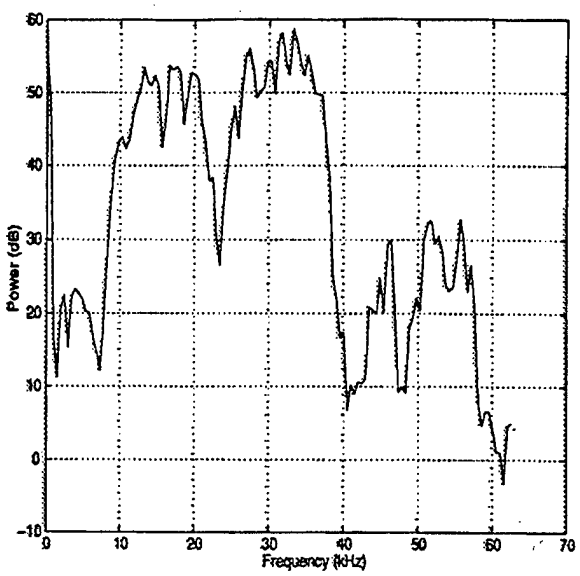

Fig. 4. Power spectrum of one ping through cable and methane gas pockets.

(column) of Fig. 2 containing the cable and methane gas pockets in cross-section. The strong peaks at various frequencies indicate that more information might be available by examining those frequencies separately.

The approach used to examine selected center frequencies is to slice the frequency spectrum into narrow bandwidths by applying a narrow-band filter, in this case a 12th-order forward-backward Butterworth filter. The filter is designed for zero phase shift and centered at the frequency of interest. Filtering the original pings and plotting the instantaneous intensity, results in profiles significantly different from that of the original data. The results for frequencies at 12.5, 19.4, 33.75, 35.0, and 55.6 kHz are shown in Fig. 5.

The profiles show a strong return of methane gas at low frequencies with an increasing return from the buried cable as the frequencies increase. In the 12.5 kHz profile, the methane gas peaks above the other returns, with an intensity of over 100. In the 19.4 kHz profile the methane gas continues to peak over 100 but the buried cable begins to peak close to 100 also. There is also a shift in the location of the methane gas responding at this frequency. At 33.75 kHz the cable peaks above 500 and the relative return from the methane gas is strongly reduced. The same occurs at 35 kHz. At 55.6 kHz the methane gas is no longer visible relative to the cable due to signal attenuation and the surface debris is the most visible due to surface reflection at the higher frequency.

The application of the filter to the entire image produces a set of images at different frequencies, shown for the area surrounding the cable cross-section in Fig. 6. These images can be considered a multispectral data set. The cable cross-section is easily seen in the 33-35 kHz frequency range and the methane is most visible at the 19.4 kHz slice.

There are several important facts to point out in these figures, one being that the peak heights are relative, not on the same scale, due to the attenuation of higher frequencies by the sediment medium. Also, because these heights are relative along the time axis, the careful selection of time and scale can be combined to enhance features in time as well as frequency. For example, by looking at a time slice of the original data around the

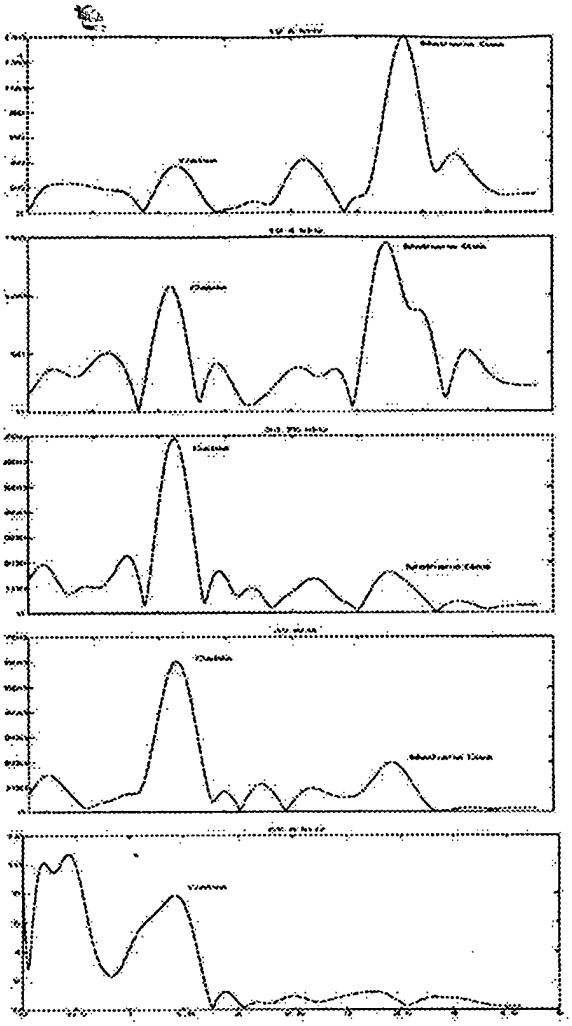

Fig. 5. Instantaneous narrow-band intensity versus meters below the seabed of a single ping at 12.5, 19.4, 33.75, 35.0, and 55.6 kHz

methane peak at 55.6 kHz, the methane can be detected as it has a stronger return than the local sediment, between 3 and 3.5 m. Thirdly, the diameter of the cable makes it almost invisible at the lower frequencies, so the knowledge of the object's size can be used to select the scale or frequency that best locates it. The combination of time and frequency together boosts the detection and identification power of an objection recognition system.

V. Time-Frequency Analysis with Wavelets

Wavelets are a function of scale and time, where scale is closely related to frequency. Two-dimensional wavelet analysis is used

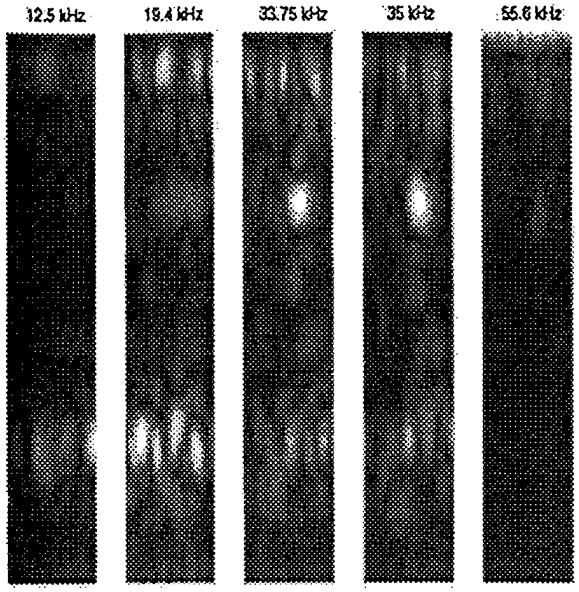

Fig. 6. Narrow-band image slices at selected frequencies.

here to decompose the original image into subimages where each pixel value represents the contribution of it's locality to a particular scale (or frequency) in time. In 2-D, the image is decomposed into horizontal, diagonal and vertical components at each level. Each level gives a low-pass component (approximation) and a high-pass component (detail). The level-1 approximation is decimated by 2 and filtered again to produce a level-2 set of high- and low-pass images.

The ASCS acoustic image should be ideal for wavelet analysis. As demonstrated above, different components in the original image have different vertical spectral response related to their composition and scale. The horizontal component of the image is strictly a function of object scale. Wavelets, by retaining both scale and frequency information should transform the image in a manner consistent with our concept of both frequency and scale. By selectively thresholding coefficients unrelated to the object in scale or frequency, we can effectively "de-noise" the data.

As an illustration of this, a fourth-order Daubechies wavelet transform was applied to

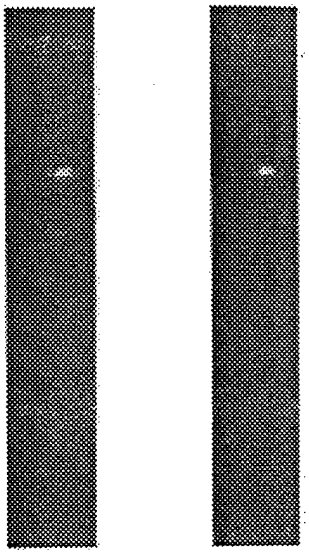

Fig. 7. The level 2 horizontal detail coefficients of the fourth order Daubechies wavelet transform and the reconstructed image after de-noising.

the original unfiltered image of Fig. 2. The results were quite good. Fig. 7 shows the level-2 horizontal detail of the original image, selected because it shows the buried cable very clearly. The wavelet coefficients may also be used to de-noise the image through thresholding of the coefficients for each level and direction, and reconstruction of the image from the coefficients below the threshold. An example of a de-noised image is shown in Fig. 7.

VI. Conclusions

In this paper, we have shown that buried objects can be detected using both multispectral and time-frequency approaches.

A frequency based approach works well in this environment where the objects respond differently to different frequencies. By slicing the spectrum into narrow bands, it is possible to distinguish objects by exploiting these differences. This frequency slicing approach has the further advantage of producing a multispectral data set which lends itself well to multivariate classification techniques.

Results thus far have shown that isolating the object in frequency and then in time and scale using wavelet analysis is an effective detection tool. Knowledge of the object's acoustic impedance properties as well it's size can be used to define the characteristics of the wavelet's order and level of decomposition to automatically look for objects at certain scales.

References

[1] Slowey, Niall C., Bryant, William R., and Lambert, Douglas N., (1996), Comparison of high-resolution seismic profiles and the geoacoustic properties of Eckernförde Bay sediments, *Geo-Marine Letters* 16:240-248.

[2] Lambert, Douglas N., Walter, Donald J., Young, David C., Richardson, Michael D., Cranford, John C., (1994), High resolution acoustic seafloor classification system for mine countermeasures operations, *Proceedings of the International Conference on Underwater Acoustics UNSW*, Australian Acoustical Society, pp 67-69.

[3] Lambert, Douglas N., Walter, Donald J., Young, David C., Griffin, Sean R., Benjamin, Kim C., (1998), Developments in acoustic sediment classification, to appear in *Proceedings of Oceans '98*.